**Geoscientific
Model Development
Discussions**

iGen: the automated generation of a parameterisation of entrainment in marine stratocumulus

D. F. Tang[1] and S. Dobbie[2]

[1]School of Mathematics, University of Manchester, Manchester, UK
[2]School of Earth and Environment, University of Leeds, Leeds, UK

Correspondence to: D. F. Tang (daniel.tang@manchester.ac.uk)

Title Page

Abstract | Introduction

Conclusions | References

Tables | Figures

◄◄ | ►►

◄ | ►

Back | Close

Full Screen / Esc

Printer-friendly Version

Interactive Discussion

Abstract

In a previous paper we described a new technique for automatically generating parameterisations using a program called iGen. iGen generates parameterisations by analysing the source code of a high resolution model that resolves the physics to be parameterised. In order to demonstrate that this technique scales up to deal with models of realistic complexity we have used iGen to generate a parameterisation of entrainment in marine stratocumulus. We present details of our technique in which iGen was used to analyse the source code of a cloud resolving model and generate a parameterisation of the mean and standard deviation of entrainment velocity in marine stratocumulus in terms of the large-scale state of the boundary layer. The parameterisation was tested against results from the DYCOMS-II intercomparison of cloud resolving models and iGen's parameterisation of mean entrainment velocity was found to be $5.27 \times 10^{-3} \pm 0.62 \times 10^{-3}\,\mathrm{m\,s^{-1}}$ compared to $5.2 \times 10^{-3} \pm 0.8 \times 10^{-3}\,\mathrm{m\,s^{-1}}$ for the DYCOMS-II ensemble of cloud resolving models.

1 Introduction

In Tang and Dobbie (2011) we described a new technique for automatically generating parameterisations. The technique begins with a high resolution model that resolves the physics to be parameterised. To this model we then add extra code to convert the inputs and outputs to those required by the parameterisation, we call this "wrapping" the model. Finally, we feed the source code of the wrapped model into a newly developed program called iGen. iGen analyses the source code, applies appropriate approximations and automatically generates the source code of a parameterisation that generally executes orders of magnitude faster than the wrapped model. In order to demonstrate iGen's ability to deal with models of realistic complexity we applied this technique to the problem of parameterising entrainment in nocturnal, non-precipitating marine stratocumulus. This involved writing a cloud resolving model of the stratocumulus topped

Full Screen / Esc

Printer-friendly Version

Interactive Discussion

boundary layer (STBL), wrapping this model so that its input was the large scale state of the STBL and its output was the entrainment velocity then feeding the source code of this model into iGen.

The large scale structure and dynamics of the STBL has been described by Lilly (1968). Typically, there is a well mixed boundary layer from the sea surface up to the cloud top within which, due to strong turbulent mixing, the total water and liquid water potential temperature is close to homogeneous. The boundary layer is capped at cloud top by a strong, well defined inversion leading up into a much warmer, dryer, stable free atmosphere. The boundary layer turbulence is driven partly by surface fluxes of heat and moisture but predominantly by strong radiative cooling at cloud top and, to a lesser extent, by radiative warming at cloud base from the warmer, underlying sea surface. This turbulence causes some of the stable, free-atmosphere air to be mixed, or "entrained" into the turbulent boundary layer. Given the rate of this entrainment, the large scale dynamics of the system is easily calculated from budgets of mass, energy and moisture. However, no analytic derivation of this entrainment rate has been found. Lilly (1968) derives upper and lower bounds and Stevens (2002) gives details of various parameterisations. However, the simulation of marine boundary layer cloud remains a large source of uncertainty and error in existing climate models. Bony and Dufresne (2005) have shown that disagreement between climate models in the simulation of marine stratocumulus is a major source of uncertainty in the estimation of climate sensitivity. They have also shown that it is in the simulation of the radiative forcing due to marine stratocumulus that climate models differ most when compared to present day observations. A more recent study (Dufresne and Bony, 2008) shows that this situation has not improved in more recent years.

2 A cloud resolving model for stratocumulus

A 2-dimensional cloud resolving model was written in C++ in order to simulate entrainment in stratocumulus under nocturnal, non-precipitating conditions. A new cloud

resolving model was written, rather than using an existing model, for two reasons: firstly, iGen can at present only analyse C++ programs, while most existing models are written in Fortran; secondly, this experiment was performed in order to test iGen, and writing a new model gave us much more freedom to see how iGen performed with different schemes and algorithms. The model was based on that of Klemp and Wilhelmson (1978) with modifications detailed in Skamrock and Klemp (1994).

A number of changes were made to the Klemp and Wilhelmson (hereafter KW) model to better suit our needs. It was found that the second-order finite difference vertical advection scheme described in KW did not cope well with the steep gradients at the inversion. This caused "ringing" effects which led to unrealistic cooling below cloudtop and heating above. To deal with this, a flux limiting advection scheme was used instead. This calculated advection as a mix between a fourth order, centred finite difference scheme and an upstream scheme. The flux limiting function used was

$$\phi(r) = \begin{cases} 0 & \text{if } r < 0 \\ 2r & \text{if } 0 \le r \le \frac{1}{2} \\ 1 & \text{otherwise.} \end{cases}$$

where r is the upwind gradient divided by the downwind gradient. Other changes are as follows:

- A more accurate version of Teten's formula was used (Emanuel, 1994).

- Temperature was stored as liquid water potential temperature.

- Liquid water was stored as total specific water content, cloud being diagnosed when this exceeds saturation.

- In order to simulate longwave radiative heating/cooling, the radiation scheme described in Larson et al. (2007) was added.

- The prognostic variable and equation for rain was removed.

– Surface fluxes of heat and moisture as a function of velocity were added.

– A homogeneous divergence was added in order to simulate large scale subsidence.

The model used a staggered grid as described in KW. The left and right boundaries were periodic in all variables. The upper and lower boundaries each lay on the vertical velocity points of the staggered grid. At the ground, horizontal and vertical velocity were constrained to zero. Other variables had the condition that $\frac{\partial}{\partial z}$ goes to zero at the ground in order to ensure zero sub-grid turbulent flux across the boundary, allowing surface fluxes to be dealt with separately. At the top of domain boundary, $v = -Dh$ where D is the large scale divergence and h is the domain height; u goes to the value of geostrophic wind; pressure perturbation from equilibrium goes to zero, liquid water and temperature go to the large-scale free atmosphere values and turbulent kinetic energy has the boundary condition $\frac{\partial K_m}{\partial z} = 0$ in order to ensure that there is no sub-grid turbulent flux of turbulence across the boundary. For all experiments, the gridbox size at the inversion was 5 m vertically and 11 m horizontally.

The surface fluxes of latent and sensible heat were calculated using a simple bulk aerodynamic formulation described in Krishnamurti and Bounoua (1995). Fluxes were added to the lowest gridbox of each column according to

$$\frac{\partial \theta}{\partial t}\bigg|_{\text{surf}} = \frac{1}{\Delta z} \|u_{10}\| C_h (T_{\text{sst}} - T) \tag{1}$$

and

$$\frac{\partial q_{\text{t}}}{\partial t}\bigg|_{\text{surf}} = \frac{1}{\Delta z} \|u_{10}\| C_q (q_{\text{sat}} - q_{\text{t}}) \tag{2}$$

where T and q_{t} are the temperature and total water of the lowest gridbox, respectively,

Δz is the height of the lowest thermodynamic grid-point and

$$u_{10} = u_x \frac{\log(\frac{10.0}{z_0})}{\log(\frac{\Delta z}{2z_0})}$$

where u_x is the horizontal velocity at the lowest gridpoint, Δz is the height of the lowest gridpoint and z_0 is the roughness length, which was taken to have a constant value of 5×10^{-4} m based on figures in Stull (1988). The exchange coefficients were set constant at $C_h = 1.4 \times 10^{-3}$ and $C_q = 1.6 \times 10^{-3}$ based on figures in Krishnamurti and Bounoua (1995).

2.1 Testing the cloud resolving model

The model was compared against observations and other cloud resolving models by performing a simulation of the first research flight of the second "dynamics and chemistry of marine stratocumulus" field study (DYCOMS-II). This case was chosen as it has been used in an intercomparison study of cloud resolving models (Stevens et al., 2005) for which a detailed specification of an idealised simulation was given, and results were collected from an ensemble of models from ten different modelling centres. This allowed our model to be compared against a wide selection of commonly used models as well as against observations.

Our model showed a longer spin-up period than the models in the intercomparison (Fig. 1) and this was attributed to the 2-dimensional turbulence of the model, compared to the 3-dimensional turbulence of the models in the intercomparison. The cascade of turbulent kinetic energy and vorticity is known to be different in 2 and 3 dimensions (Kraichnan, 1967). During this spin-up period, the low turbulent kinetic energy led to low entrainment and so the prescribed large scale subsidence caused the cloudtop to descend. In order to account for this descent during the spin-up period, the initial cloudtop height was raised by 10 m, this had the effect of bringing the cloudtop height in-line with the other models at 2-h into the simulation when the spin-up period was over.

From 2-h into the simulation to the end of the simulation the model was in good agreement with both observation and the models of the intercomparison. Cloudtop height, and therefore entrainment, was very close to the ensemble average (see Fig. 2). Cloudbase height was also very close to the ensemble average (see Fig. 3).

3 Wrapping the CRM to calculate entrainment

The cloud resolving model was wrapped so that its input was the large scale state of the STBL. This was specified as the variables

$q_{l,ct}$ Specific liquid water content at cloud top

Δq_t Jump in specific total water at cloud top

ΔB Jump in buoyancy at cloud top

F_0 Down-welling radiation just above cloud top

F_1 Up-welling radiation just below cloud base

The ranges of the large scale variables over which the parameterisation should be valid were calculated from the results of a number of field campaigns and idealised cases of nocturnal marine stratocumulus as shown in Table 1.

Based on these results, the ranges used for iGen's analysis of the wrapped model were:

– $1 \times 10^{-4} \leq q_{l,ct} \leq 1 \times 10^{-3}\,\mathrm{Kg\,Kg^{-1}}$

– $-8.0 \times 10^{-3} \leq \Delta q_t \leq -2.0 \times 10^{-3}\,\mathrm{Kg\,Kg^{-1}}$

– $0.065 \leq \Delta B \leq 0.5\,\mathrm{m\,s^2}$

– $20 \leq F_0 \leq 110\,\mathrm{W\,m^2}$

- $7 \leq F_1 \leq 33 \, \mathrm{W \, m^2}$.

Given the 5 large scale variables, it was found that the dependency of entrainment on boundary layer temperature was very weak over the range of values we expect to experience (see Sect. 4). In light of this insensitivity it was decided to set average
5 boundary layer liquid water potential temperature to 290 K, the centre of its range. Sea surface temperature was held fixed at 291 K. Atmospheric pressure at sea level was assumed to be $1 \times 10^5 \, \mathrm{N \, m^2}$.

The initial state of the atmosphere was based on the large scale variables and consisted of a homogeneous boundary layer and homogeneous free atmosphere sepa-
10 rated by a linear transition of 25 m height. Initial velocities were zero everywhere and there was no sub-grid turbulent kinetic energy. Pressure was initialised to the hydrostatic value. In order to break symmetry, a random perturbation of ±0.0025 K was added to each gridbox below 100 m and within 100 m below the inversion. Geostrophic winds were not included for the same reason as given in Moeng et al. (1996): if we
15 are to include geostrophic winds, this raises the question of the orientation of the 2-D domain in relation to the wind direction. Since roll motions tend to be aligned closely to the wind direction, the natural choice would be perpendicular to the wind direction, meaning no geostrophic wind across the domain.

The simulation ran for 6 simulated hours, over this time the large scale state was
20 held constant. In order to do this, a set of fluxes were calculated every 12 simulated seconds and added at each timestep. The boundary layer height was kept constant by adding a homogeneous, large-scale divergence. This was calculated according to:

$$\nabla \cdot v = \frac{m_\mathrm{d} + \frac{h - H}{5 \Delta t}}{H}$$

where m_d is the gradient of the least squares linear fit to the total entrainment over
25 the duration of the simulation so far, h is the measured height of the boundary layer, Δt is the time between updates (12 s) and H is the required height. The height of the

boundary layer was defined to be the average height of the isoline of total water content half way between the large-scale boundary layer and free atmosphere values.

In order to keep boundary layer temperature and moisture constant a total water flux and temperature flux was added. Total water flux was added to the sub-cloud portion of the boundary layer. This included a flux that tended to homogenise the field and was calculated at each gridpoint as

$$\frac{\partial q_t}{\partial t} = m_q + \frac{q_{tbl} - q_t}{8\Delta t}$$

where m_q is the gradient of the least squares linear fit of the total flux from the beginning of the simulation, q_{tbl} is the large-scale total water in the boundary layer and q_t is the field of actual total water. The homogenisation is not physical but is justified on the grounds that we want to find a formula for entrainment in order to close the large scale dynamics of the boundary layer. However, the large scale dynamics is only valid under the assumption of a homogeneous boundary layer so we are merely enforcing the assumption made by the large scale dynamical view.

The flux of liquid water potential temperature was calculated so as to add a constant buoyancy to the whole boundary layer from the ground up to the isoline of temperature half way between the large-scale boundary layer and free atmosphere values. In this way, the dynamics of the boundary layer is not affected by the flux. The calculation was performed by first calculating a homogeneous buoyancy flux

$$\frac{\partial B}{\partial t} = m_b + \frac{\theta_{lbl} - \bar{\theta}_l}{30\theta_{lbl}\Delta t}$$

where $\bar{\theta}_l$ is the average liquid water temperature between 200 m and 100 m below cloud top and m_b is the gradient of the least squares linear fit of the total flux of buoyancy since the beginning of the simulation.

The flux of liquid water potential temperature necessary to achieve a given change in buoyancy ΔB over a single timestep, given a change in total water Δq_t, was calculated

and added at the end of each timestep. The change in liquid water potential temperature $\Delta\theta_l$ at each gridbox was calculated using the following procedure: In the absence of liquid water

$$\Delta\theta_{l,\mathrm{dry}} = \theta_{\mathrm{lbl}}(\Delta B - 0.61\Delta q_t)\Delta t$$

5   in the presence of liquid water

$$\Delta\theta_{l,\mathrm{wet}} = \theta_{\mathrm{lbl}}\left(\Delta B - \Delta q_t\left(\frac{\gamma}{\theta_{\mathrm{lbl}}} - 1\right)\left(1 - \frac{\partial q_{\mathrm{sat}}}{\partial q_t}\right)\right)$$

and $\frac{\partial q_{\mathrm{sat}}}{\partial q_t}$ is the rate of change of saturation with q_t at constant θ_l. In the case that the flux causes a transition between clear sky and cloud, it is necessary to calculate the fraction of buoyancy and q_t change that occurs in cloud and the fraction in clear sky
10   and to add these contributions separately. When going from clear sky to cloudy, the fraction in clear sky is given by

$$m = \frac{q_{\mathrm{sat}} - q_t}{\Delta q_t - \frac{\partial q_{\mathrm{sat}}}{\partial \theta_l}\Delta\theta_{l,\mathrm{dry}}}$$

where $\frac{\partial q_{\mathrm{sat}}}{\partial \theta_l}$ is the rate of change of saturation with θ_l at constant q_t. When going from cloudy to clear, the fraction in cloudy sky is

15   $$m = \frac{q_t - q_{\mathrm{sat}}}{\left(1.0 - \frac{\partial q_{\mathrm{sat}}}{\partial q_t}\right)\Delta q t - \frac{\partial q_{\mathrm{sat}}}{\partial \theta_l}\Delta\theta_{l,\mathrm{wet}}}\ .$$

3.1   Wrapped model output

The output of the wrapped model was the entrainment velocity averaged over the final 4 simulated hours of a 6 h simulation. Since the entrainment is caused by the action of a number of random, turbulent events, the exact details of which we cannot predict
20   from the large scale state, and since we are averaging over a finite area and time,

there is a certain amount of uncertainty associated with the mean entrainment. This uncertainty can be split into two types. On the one hand, the parameterisation is to be used to calculate entrainment over a finite area and timestep so we would expect there to be an intrinsic uncertainty in the entrainment due to the finite number of entrainment events over which the parameterisation is supposed to be averaging. This uncertainty should be included in the parameterisation, making it a stochastic parameterisation. On the other hand, there is the uncertainty in the mean entrainment associated with the finite (4 h) time over which the mean was calculated by the wrapped model.

Both these uncertainties come from our lack of knowledge of the small scale state of the system given only the large scale state. In order to show that this uncertainty is significant, a numerical experiment was performed on the wrapped model to test the sensitivity of entrainment rate to an initial random perturbation of ± 0.0025 K to each gridbox in the lowest 100 m of the boundary layer and within 100 m below the inversion. The large-scale state was chosen to be around the centre of the expected ranges of each value:

Boundary layer q_t $= 8 \times 10^{-3}$ Kg Kg^{-1}

$\Delta \theta_l$ at inversion $= 8.5$ K

Δq_t at inversion $= -6 \times 10^{-3}$ Kg Kg^{-1}

Net radiation flux above inversion $= -55$ W m^{-2}

Net radiation flux at cloud base $= 22$ W m^{-2}

The domain size was 1166 m horizontally and 770 m vertically. The inversion height was 600 m above the bottom of the domain.

Six simulations were made with random perturbations provided by the C++ `rand()` function, seeded at the beginning of the simulation by the current state of the computer's internal clock. The fluxes of heat and moisture which keep the boundary layer at a constant large scale state were turned off in order to discount them as the source

of sensitivity. The resulting total entrainment of the simulations are shown in Fig. 4. After 6 h there was a 10% spread in total entrainment, showing that there is significant sensitive dependence on initial conditions under these conditions.

Debugging showed no memory leaks or out-of-range references in the program, which could have caused the differing behaviour. Running the simulations with the same random seed at various times and on different computers always returned the same result. Simulations were also made with the large-scale divergence feedback turned off in order to discount this as a possible source of sensitivity. Results still showed sensitivity to initial conditions. Different domain geometries did not show any overall reduction in sensitivity. Sensitivity was reduced to around 5% when the large-scale boundary layer state was held constant by turning on the fluxes of heat and moisture.

In order to deal with this uncertainty we choose to have the wrapped model also calculate the standard deviation of the entrainment. This was calculated from averages taken over contiguous 216 s intervals. The standard deviation in the mean is easily calculated as $\frac{\sigma}{\sqrt{N-1}}$ where σ is the standard deviation of the 216 s samples and N is the number of samples. If the entrainment is assumed to result from a large number of small, independent entrainment events then we would expect the standard deviation, when averaged over a time T and an area A, to scale according to $\sigma \propto A^{-\frac{1}{2}} T^{-\frac{1}{2}}$. However, to calculate the constant of proportionality from our samples we must account for the added complication of extrapolating from our 2 dimensional model to 3 dimensional reality. A plausible way of doing this would be to say

$$\sigma = \sigma_{2d} \sqrt{\frac{lwt}{AT}}$$

where σ_{2d} is the standard deviation of the samples, l is a characteristic length scale of the entrainment, $w = 1166$ m is the width of the domain of the wrapped model and $t = 216$ s is the duration of each sample.

A reasonable figure for the characteristic length scale can be calculated by noting that since the entrainment predominantly occurs in only one direction, each entrainment event must predominantly mix free atmosphere air into the boundary layer. For this to be the case, the mean entrainment must remain larger than the standard deviation, so the scale of the process of entrainment must be no smaller than that where the standard deviation of each event equals its mean. Taking data from a 15 h simulation with the same large scale state as above and supposing a characteristic velocity of $1 \, \mathrm{m\,s^{-1}}$ gives a characteristic length scale of 15 m.

4 Sensitivity of entrainment to domain geometry

Numerical experiments were performed to find the sensitivity of the wrapped model output to the domain geometry of the CRM. The reference geometry was 770 m vertical by 1166 m horizontal, with the inversion at 600 m. The following perturbations to the reference geometry were tested:

– 5500 m horizontal

– 1200 m vertical

– inversion at 1100 m with 1270 m vertical domain.

In all cases, the values of the large scale inputs to the model were chosen to be as follows:

$$q_{l,ct} = 5.5 \times 10^{-4} \, \mathrm{Kg\,Kg^{-1}}$$

$$\Delta q_t = -6.0 \times 10^{-3} \, \mathrm{Kg\,Kg^{-1}}$$

$$\Delta B = 0.215 \, \mathrm{m\,s^{-2}}$$

$$F_0 = 55 \, \mathrm{W\,m^{-2}}$$

$$F_1 \quad = 22\,\mathrm{W\,m^{-2}}$$

$$\theta_{\mathrm{l,bl}} \quad = 290\,\mathrm{K}$$

$$\Delta T_{\mathrm{sst}} \quad = 1\,\mathrm{K}.$$

In addition, sensitivity to boundary layer liquid water potential temperature (with all other variables fixed) was tested by performing a simulation at 295 K, the upper limit of the expected range.

The simulations lasted 15 simulated hours and the initial spin-up period was 9 h. The resulting entrainments of the simulations are shown in Fig. 5 as a function of time. The gradients of the least squares fits are shown in Table 2. The results show that the reference geometry, although small, gives values for entrainment that agree well with different geometries, considering the intrinsic standard deviation of entrainment.

5 Results

iGen was left running for 28 days on a desktop computer with 1.8 GHz Intel Core-Duo. On return, the analysis had terminated and reported a 10th order total-degree polynomial for both mean entrainment and standard deviation. The resulting mean entrainment polynomial was shown to have converged by converting it to Chebyshev form and forming a "high-order polynomial" consisting of all the highest order terms (i.e. those for which all other terms have at least one variable of lower degree). As the polynomial converges, we would expect the high-order polynomial to reduce in amplitude to the level of "noise" due to the standard deviation in the mean. At this point we would expect the amplitude of the high-order polynomial to lie within 0.674 standard deviations of the mean 50% of the time. The high-order polynomial and standard deviation of the mean were evaluated at 10 000 randomly chosen points in the input domain. The proportion of points for which the high-order polynomial was found to lie within 0.674

standard deviations was found to be 49.85%, so the polynomial was taken to have converged.

The polynomials for mean and standard deviation that resulted from the analysis are given in the supplementary files. The polynomials are expanded in the Chebyshev basis, so x^n should be taken to mean the nth Chebyshev polynomial defined as $\cos(n\cos^{-1}(x))$. These can easily be converted into a program that evaluates the mean and standard deviation at any point in just over 2000 multiplications and additions by using Horner form evaluation. Approximations that require fewer operations can easily be created by Chebyshev approximation, by finding the minimax polynomial fit using Remez' algorithm (Press et al., 2007) or by finding the least squares fit by solving the appropriate set of linear equations (Press et al., 2007).

The polynomials were tested against the ensemble of cloud resolving models used in the DYCOMS-II intercomparison (Stevens et al., 2005). The ensemble-average large-scale state for the final hour of the simulations was used as input to the polynomial, and the entrainment over 1 h was predicted to be $5.27 \times 10^{-3} \pm 0.62 \times 10^{-3}\,\mathrm{m\,s^{-1}}$. This compares very well with the ensemble average of the CRM's entrainment rate which was $5.2 \times 10^{-3} \pm 0.8 \times 10^{-3}\,\mathrm{m\,s^{-1}}$.

6 Conclusions

iGen has analysed the source code of a wrapped, high-resolution cloud resolving model of entrainment in marine stratocumulus and from this has derived a parameterisation of entrainment in terms of the large scale state of the boundary layer. This demonstrates iGen's ability to create parameterisations from models of realistic complexity.

Although the primary purpose of creating this parameterisation was as a demonstration of iGen, the resulting parameterisation shows good agreement with an ensemble of cloud resolving models and could be used in a climate model. The biggest limitation of the parameterisation is that it is based on a 2-dimensional simulation and, as

already mentioned, 2-dimensional turbulence is known to have different characteristics from its 3-dimensional counterpart. The similarity in results between our model and the 3-dimensional models in the DYCOMS-II case, however, would suggest that this may not adversely affect entrainment rates. This is in line with Moeng et al. (1996) who also found a similar insensitivity of entrainment rate to model dimensionality. This insensitivity may be a result of the finite resolution of the model, it is not clear whether the 5 m resolution of our cloud resolving model is enough to capture the processes involved in entrainment. It would be worthwhile repeating this experiment with a higher grid resolution and in 3-dimensions. It would also be worthwhile treating boundary layer temperature and sea surface temperature as input variables in order to formally show their functional role in entrainment.

Despite these limitations, we have shown that iGen is capable of generating parameterisations from models of realistic complexity and that it has the potential to become a valuable tool in model development. We have also presented a parameterisation of entrainment in nocturnal marine stratocumulus which could be incorporated into the boundary layer parameterisation scheme of a climate model.

**Supplementary material related to this article is available online at:
http://www.geosci-model-dev-discuss.net/4/971/2011/
gmdd-4-971-2011-supplement.zip**.

References

Albrecht, B. A., Randall, D. A., and Nicholls, S.: Observations of marine stratocumulus clouds during FIRE, B. Am. Meteorol. Soc., 69, 618–626, 1988. 989

Bony, S. and Dufresne, J.: Marine boundary layer clouds at the heart of tropical cloud feedback uncertainties in climate models, Geophys. Res. Lett., 32, L20806, doi:10.1029/2005GL023851, 2005. 973

Bretherton, C. S. and Pincus, R.: Cloudiness and marine boundary layer dynamics of the ASTEX Lagrangian experiments. Part I: Synoptic setting and vertical structure, J. Atmos. Sci., 52, 2707–2723, 1995. 989

Bretherton, C. S., Austin, P. and Siems, S. T.: Cloudiness and marine boundary layer dynamics in the ASTEX Lagrangian experiments. Part II: Cloudiness, drizzle, surface fluxes and entrainment, J. Atmos. Sci., 52, 2724–2735, 1995. 989

Dufresne, J. L. and Bony, S.: An assessment of the primary sources of spread of global warming estimates from coupled atmosphere-ocean models, J. Climate, 21, 5135–5144, 2008. 973

Emanuel, K. A.: Atmospheric Convection, Oxford University Press, Oxford, 1994. 974

Klein, S. A. and Hartmann, D. L.: The seasonal cycle of low stratiform clouds, J. Climate, 6, 1587–1606, 1993. 989

Klemp, J. B. and Wilhelmson, R. B.: The simulation of three-dimensional convective storm dynamics, J. Atmos. Sci., 35, 1070–1096, 1978. 974

Kraichnan, R. H.: Inertial ranges in two-dimensional turbulence, Phys. Fluids, 10, 1417–1423, 1967. 976

Krishnamourti, T. N. and Bounouna, L.: An Introduction to Numerical Weather Prediction Techniques, CRC Press, Florida, 1995. 975, 976

Larson, V. E., Kotenberg, K. E., and Wood, N. B.: An analytic longwave radiation formula for liquid layer clouds, Mon. Weather Rev., 135, 689–699, 2007. 974

Lilly, D. K.: Models of cloud-topped mixed layers under a strong inversion, Q. J. Roy. Meteorol. Soc., 94, 292–309, 1968. 973

Moeng, C. H., Cotton, W. R., Bretherton, C., Chlond, A., Khairoutdinov, M., Krueger, S., Lewellen, W. S., Macvean, M. K., Pasquier, J. R. M., Rand, H. A., Siebesma, A. P., Stevens, B., and Sykes, R. I.: Simulation of a stratocumulus-topped planetary boundary layer: intercomparison among different numerical codes, B. Am. Meteorol. Soc., 77, 261–278, 1996. 978, 986, 989

Press, W. H., Teukolsky, S. A., Vetterling, W. T., and Flannery, B. P.: Numerical Recipes: the Art of Scientific Computing, 3rd Edn., Cambridge University Press, Cambridge, UK, 2007. 985

Skamrock, W. C. and Klemp, J. B.: Efficiency and accuracy of the Klemp-Wilhelmson time-splitting technique, Mon. Weather Rev., 122, 2623–2630, 1994. 974

5 Stevens, B.: Entrainment in stratocumulus-topped mixed layers, Q. J. Roy. Meteorol. Soc., 128, 2663–2690, 2002. 973

Stevens, B., Moeng, C., Ackerman, A. S., Bretherton, C. S., Chlond, A., DeRoode, S., Edwards, J., Golaz, J., Jiang, H., Khairoutdinov, M., Kirkpatrick, M. P., Lewellen, D. C., Lock, A., Muller, F., Stevens, D. E., Whelan, E., and Zhu, P.: Evaluation of large-eddy simulations via obser-
10 vations of nocturnal marine stratocumulus, Mon. Weather Rev., 133, 1443–1462, 2005. 976, 985, 989, 991

Stull, R. B.: An Introduction to Boundary Layer Meteorology, Kluwer Academic Publishers, Netherlands, 1988. 976

Tang, D. F. and Dobbie, S.: iGen: a program for the automated generation of models and pa-
15 rameterisations, Geosci. Model Dev. Discuss., 4, 843–868, doi:10.5194/gmdd-4-843-2011, 2011. 972

iGen: the automated parameterisation of entrainment in stratocumulus

D. F. Tang and S. Dobbie

Title Page

Abstract | Introduction

Conclusions | References

Tables | Figures

◄ | ►

◄ | ►

Back | Close

Full Screen / Esc

Printer-friendly Version

Interactive Discussion

Table 1. The ranges of large scale boundary layer values found in various published sources.

Reference	$\theta_{l,bl}$ (K)	$\Delta\theta_l$ (K)	$q_{t,bl}$ (kg kg^{-1})	Δq_t (kg kg^{-1})	H (m)	F_0 (W m^{-2})	$q_{l,ct}$ ($\times 10^{-4}$ kg kg^{-1})
Stevens et al. (2005)	289.0	8.5	9.0	−7.5	840	70	4.75
Moeng et al. (1996)	288.0	5.5	8.0	−4.6	662.5 : 690	15 : 30	4.4 : 6.6
Albrecht et al. (1988)	289	5 : 11	7.0	−6.0	500 : 1100	40	−
Bretherton and Pincus (1995)	292.0	2 : 4	10.0	−5 : −8	435 : 1358	−	2.2 : 5.2
Bretherton et al. (1995)	290 : 294.5					−	
Bretherton and Pincus (1995)	291 : 292	11	9.0	−3 : −8	1800	−	0 : 10.0
Bretherton et al. (1995)	291 : 293.5						
Klein and Hartmann (1993)						100	

Table 2. The least squares fit of the rate of entrainment for different domain geometries.

Simulation	Entrainment ($\mathrm{m\,s^{-1}}$)
Reference	7.45×10^{-3}
Wide	7.28×10^{-3}
Free atmosphere	7.59×10^{-3}
1100 m boundary layer	7.31×10^{-3}
$\theta_{l,bl} = 295\,\mathrm{K}$	7.50×10^{-3}

Fig. 1. Cloudtop height of DYCOMS-II simulation: solid line shows results from our 2-D CRM. The inner error bars show the first and third quartiles of the ensemble of models in the Stevens et al. (2005) intercomparison, the outer error bars show the maximum and minimum values of the ensemble. The mid-points of the error bars are marked by crosses and plus signs, respectively.

Fig. 2. DYCOMS-II simulation: cloudtop height from 2 h into the simulation. The solid line shows the results from the 2-D CRM. Inner error bars show the first and third quartiles of the ensemble of intercomparison models, the outer error bars shows the maximum and minimum values of the ensemble.

Cloudbase height

Fig. 3. DYCOMS-II simulation: cloudbase height from 2 h into the simulation. The solid line shows the results from the 2-D CRM. Inner error bars show the first and third quartiles of the ensemble of intercomparison models, the outer error bars shows the maximum and minimum values of the ensemble.
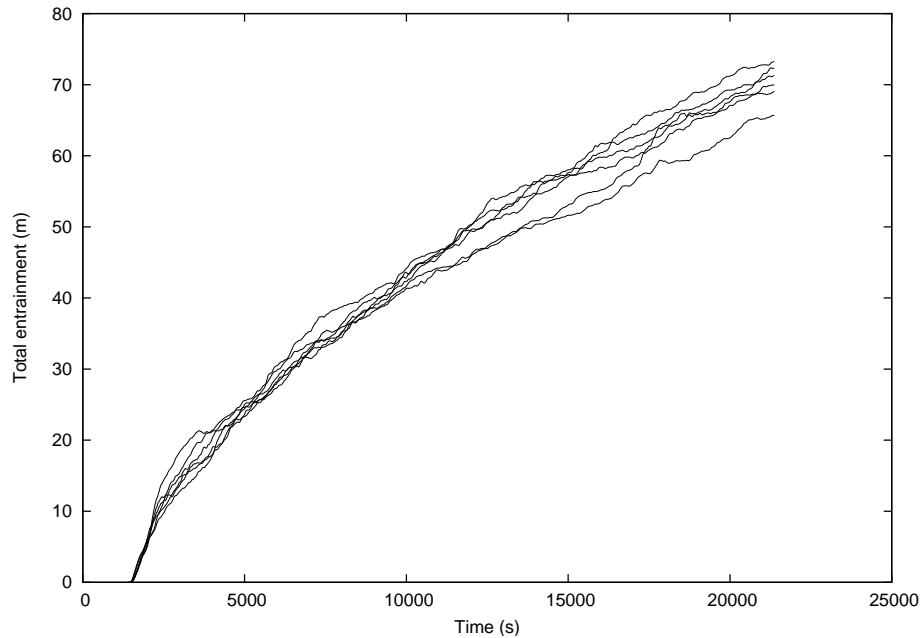
Fig. 4. Total entrainment against simulated time for six simulations differing only in a 0.0025 K perturbation to the initial conditions.

Title Page

Abstract   Introduction

Conclusions   References

Tables   Figures

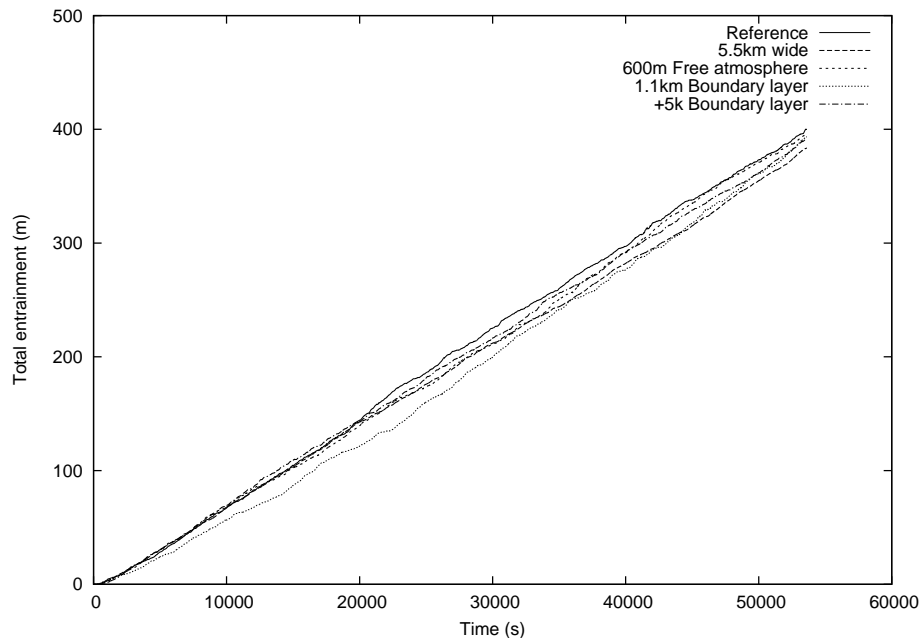◄   ►◄

◄   ►

Back   Close

Full Screen / Esc

Printer-friendly Version

Interactive Discussion

Fig. 5. Entrainment of the CRM for different geometries and different boundary layer temperature.